

Supporting Information

Role of Anderson Rule in Determining Electronic, Optical and Transport Properties of Transition-metal Dichalcogenides Heterostructures

Ke Xu¹, Yuanfeng Xu¹, Hao Zhang^{1†}, Bo Peng¹, Hezhu Shao^{2‡}, Gang Ni¹, Jing Li¹, Mingyuan Yao¹, Hongliang Lu³, Heyuan Zhu^{1¶} and Costas M. Soukoulis^{4,5}

¹*Department of Optical Science and Engineering,*

Key Laboratory of Micro and Nano Photonic Structures (MoE) and Key Laboratory for Information Science of Electromagnetic Waves (MoE),

Fudan University, Shanghai 200433, China.

²*Ningbo Institute of Materials Technology and Engineering,*

Chinese Academy of Sciences, Ningbo 315201, China

³*State Key Laboratory of ASIC and System,*

Institute of Advanced Nanodevices, School of Microelectronics,

Fudan University, Shanghai 200433, China

⁴*Department of Physics and Astronomy and Ames Laboratory,*

Iowa State University, Ames, Iowa 50011, USA

⁵*Institute of Electronic Structure and Laser (IESL),*

*FORTH, 71110 Heraklion, Crete, Greece**

(Dated: August 21, 2018)

TABLE S1. Monolayer MX₂ system and band gaps, optimized lattice constant a (Å), Young's modulus $Y(N/m)$ and Poisson's ratio ν , electron and hole effective masses along armchair direction, deformation potential constants for CBM and VBM along armchair direction. Other theoretical data are also listed in parentheses for comparison

System	E_g^{PBE} (eV)	$a(\text{\AA})$	$Y(N/m)$	ν	$m_e^*(m_0)$	$m_h^*(m_0)$	D_l^e	D_l^h
MoS ₂	1.67 (1.67 ¹)	3.18 (3.18 ¹)	125.91 (127.3 ¹)	0.25 (0.24 ¹)	0.48 (0.55 ²)	0.59 (0.56 ²)	2.91	2.48
MoSe ₂	1.44 (1.44 ¹)	3.32 (3.32 ¹)	101.20 (104.8 ¹)	0.23 (0.23 ¹)	0.59 (0.49 ²)	0.68 (0.61 ²)	2.57	2.31
MoTe ₂	1.08 (1.07 ¹)	3.55 (3.55 ¹)	78.52 (79.9 ¹)	0.24 (0.24 ¹)	0.61 (0.65 ²)	0.72 (0.64 ²)	2.06	1.95
WS ₂	1.81 (1.82 ¹)	3.18 (3.18 ¹)	141.25 (141.9 ¹)	0.21 (0.21 ¹)	0.33 (0.46 ²)	0.42 (0.42 ²)	2.23	2.19
WSe ₂	1.54 (1.54 ¹)	3.31 (3.32 ¹)	120.73 (114.4 ¹)	0.23 (0.19 ¹)	0.36 (0.48 ²)	0.46 (0.44 ²)	2.67	2.34
WTe ₂	1.06 (1.05 ¹)	3.55 (3.55 ¹)	90.57 (88.8 ¹)	0.20 (0.17 ¹)	0.29 (0.28 ³)	0.39 (0.54 ³)	1.95	2.69

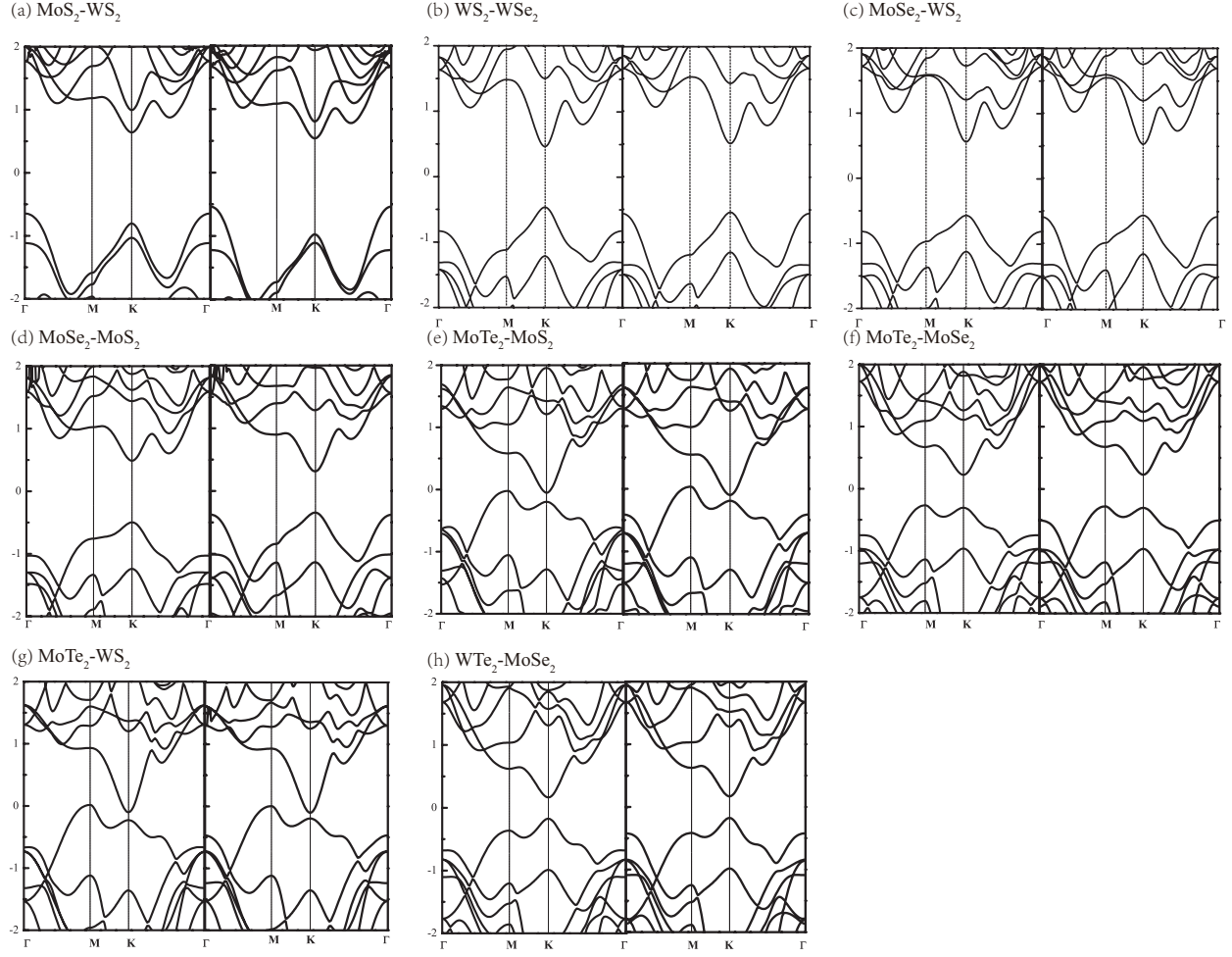


FIG. S1. Band structures of the vdW MX_2 heterostructures with AA and AB stacking types.

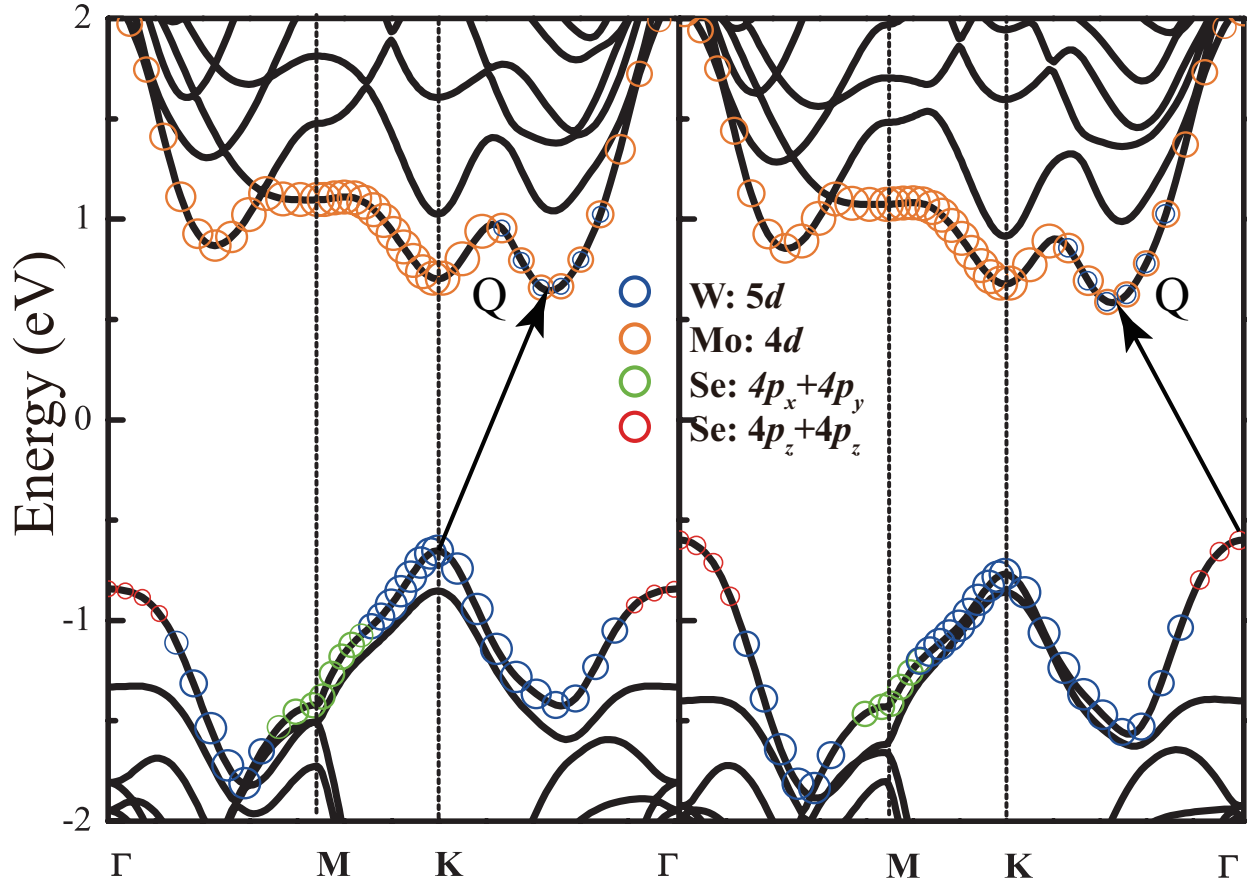


FIG. S2. Band structures of the AA and AB stacking vdW MoSe₂-WSe₂ heterostructures and atomic orbital weights in the energy bands. The blue and orange circles represent *d* orbitals of the cations. The green and red circles represent *p*_x+*p*_y and *p*_z orbitals of the anions, respectively. The size of each circle is proportional to the weight of the atomic orbital.

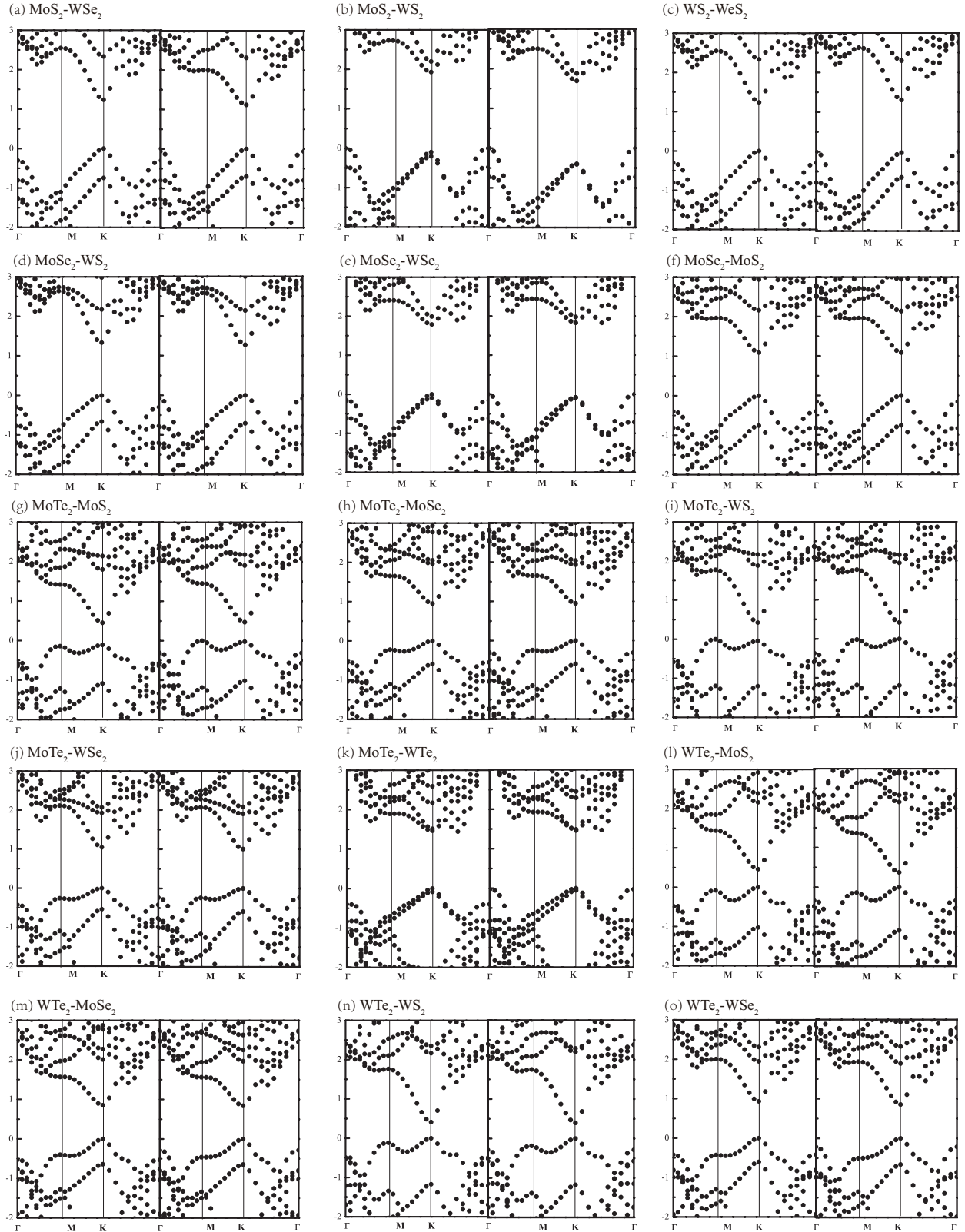


FIG. S3. Band structures under HSE06 hybrid functional of the vdW MX_2 heterostructures with AA and AB stacking types.

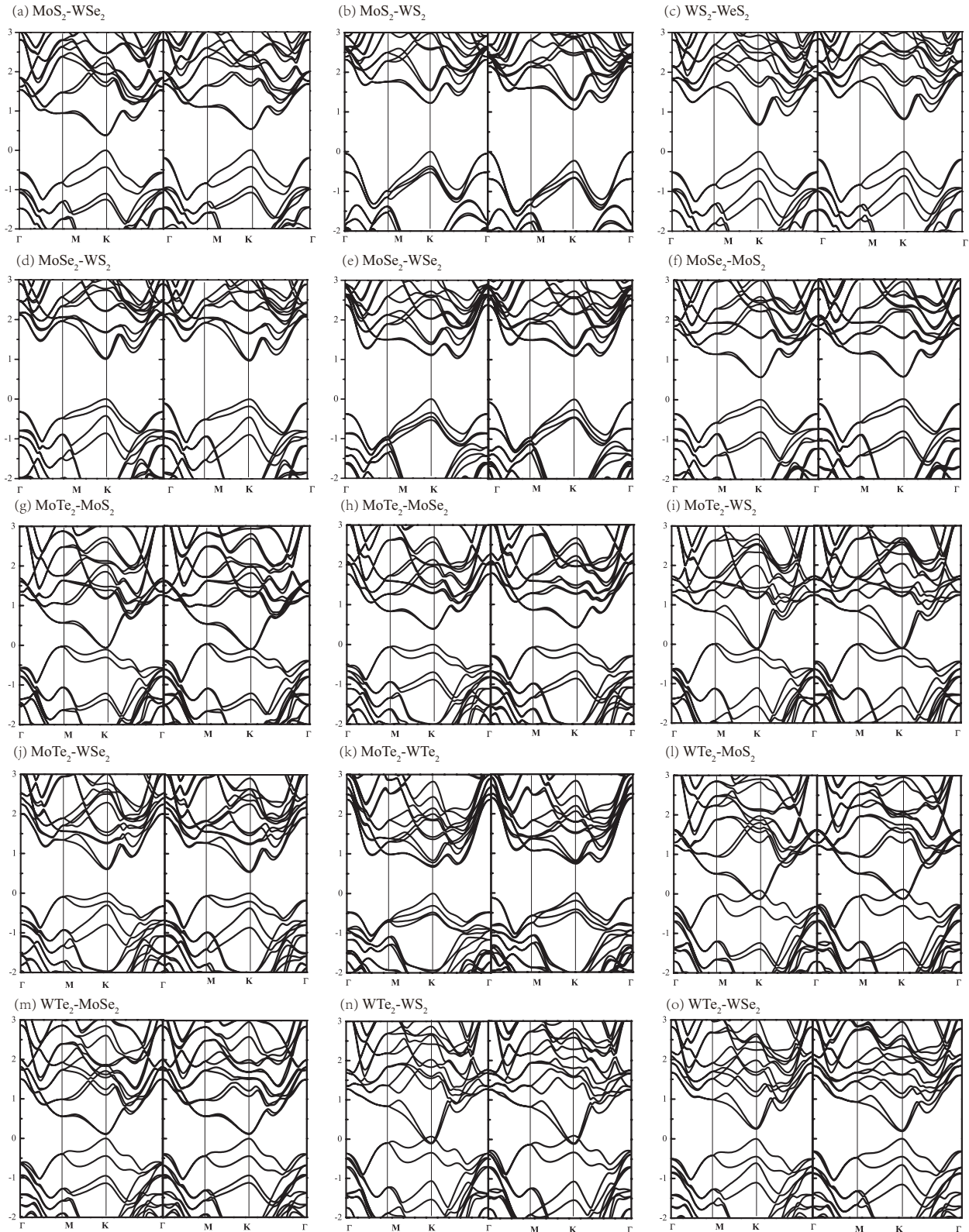


FIG. S4. Band calculations with SOC of the vdW MX₂ heterostructures with AA and AB stacking types.

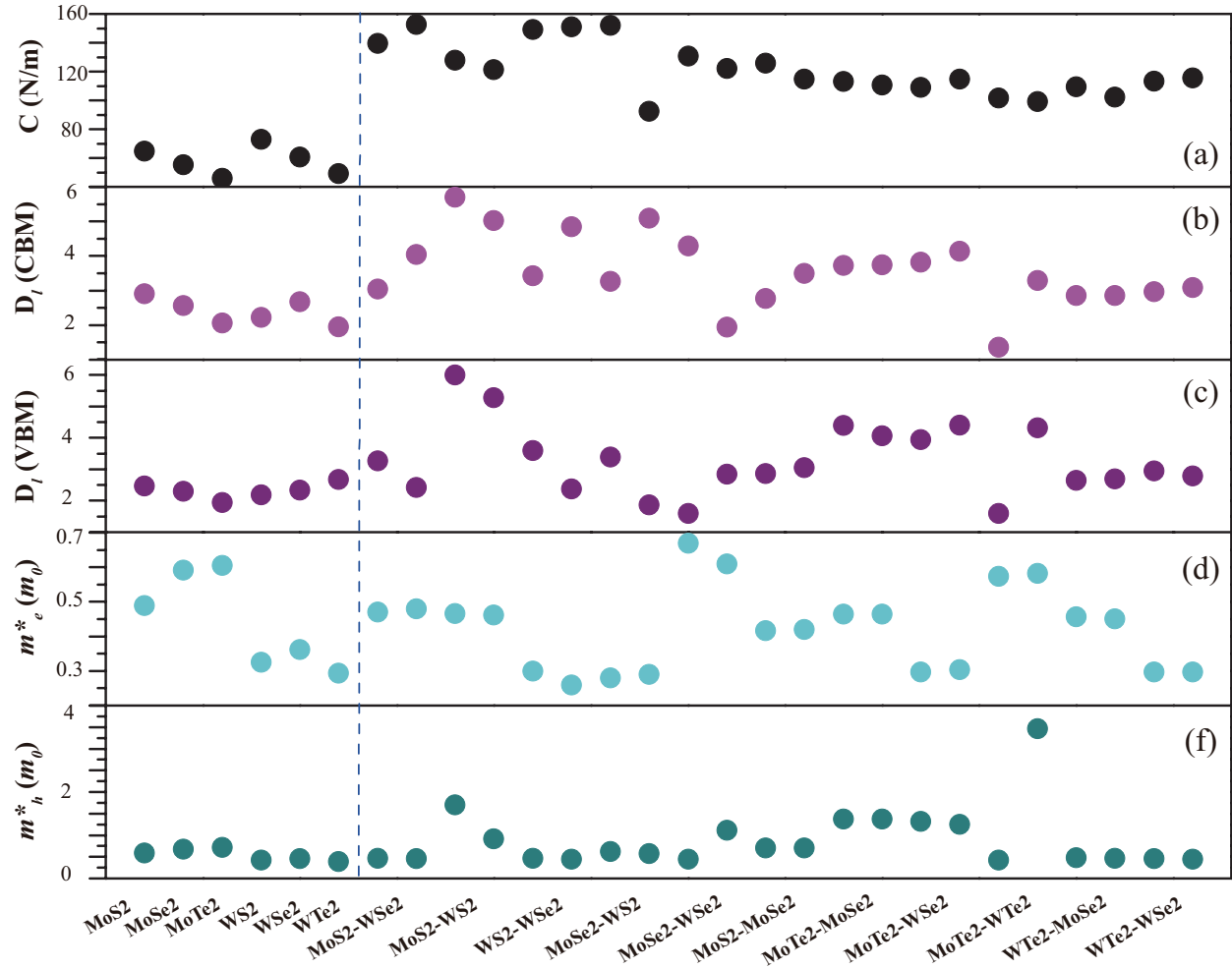


FIG. S5. The calculations of the three factors (elastic modulus , deformation potential (DP) constant and the effective mass) for carrier mobility along armchair of monolayer MX_2 and the vdW MX_2 heterostructures.

TABLE S2. The calculated elastic constants of the vdW MX₂ heterostructures in units of N/m calculated using PBE functional and the formation energy.

System	Stacking type	C ₁₁	C ₁₂	C ₄₄	E(eV)
MoS ₂ -WSe ₂ (II)	AA	232.54	58.98	90.24	-0.56
	AB	228.02	62.25	90.46	-0.54
MoS ₂ -WS ₂ (II)	AA	257.57	64.42	98.00	-0.65
	AB	257.34	62.78	97.76	-0.63
WS ₂ -WSe ₂ (II)	AA	245.38	63.24	91.64	-0.68
	AB	242.76	62.34	88.23	-0.65
MoSe ₂ -WS ₂ (II)	AA	288.16	88.2	87.63	-0.56
	AB	302.74	95.42	88.49	-0.54
MoSe ₂ -WSe ₂ (II)	AA	236.36	64.28	86.74	-0.60
	AB	230.66	64.86	87.29	-0.58
MoS ₂ -MoSe ₂ (II)	AA	249.52	64.63	90.33	-0.44
	AB	248.03	66.20	91.87	-0.41
MoTe ₂ -MoS ₂ (II)	AA	225.38	80.23	80.32	-0.13
	AB	223.12	76.54	72.74	-0.10
MoTe ₂ -MoSe ₂ (II)	AA	204.60	63.71	77.39	-0.15
	AB	214.13	54.10	79.79	-0.14
MoTe ₂ -WS ₂ (II)	AA	223.87	62.95	80.08	-0.02
	AB	216.66	67.13	74.91	-0.01
MoTe ₂ -WSe ₂ (I)	AA	199.87	56.85	77.00	-2.12
	AB	206.26	48.81	79.64	-2.19
MoTe ₂ -WTe ₂ (II)	AA	160.89	62.87	63.87	-0.30
	AB	180.83	40.33	69.68	-0.28
WTe ₂ -MoS ₂ (III)	AA	176.32	35.11	72.56	-0.05
	AB	205.09	57.29	74.07	-0.01
WTe ₂ -MoSe ₂ (II)	AA	198.64	54.23	78.39	-0.27
	AB	206.41	45.45	79.78	-0.26
WTe ₂ -WS ₂ (III)	AA	197.09	39.93	79.21	-0.19
	AB	254.30	73.13	80.47	-0.17
WTe ₂ -WSe ₂ (I)	AA	189.41	63.15	75.81	-0.39
	AB	207.91	45.92	80.74	-0.38

REFERENCE

* †zhangh@fudan.edu.cn; ‡hzshao@nimte.ac.cn; ¶hyzhu@fudan.edu.cn

- ¹ Fan Zeng, Wei-Bing Zhang, and Bi-Yu Tang. Electronic structures and elastic properties of monolayer and bilayer transition metal dichalcogenides MX₂ (m = mo, w; x = o, s, se, te): A comparative first-principles study. *Chinese Physics B*, 24(9):097103, sep 2015.
- ² Filip A. Rasmussen and Kristian S. Thygesen. Computational 2d materials database: Electronic structure of transition-metal dichalcogenides and oxides. *The Journal of Physical Chemistry C*, 119(23):13169–13183, jun 2015.
- ³ H. Y. Lv, W. J. Lu, D. F. Shao, Y. Liu, S. G. Tan, and Y. P. Sun. Perfect charge compensation in WTe₂ for the extraordinary magnetoresistance: From bulk to monolayer. *EPL (Europhysics Letters)*, 110(3):37004, may 2015.